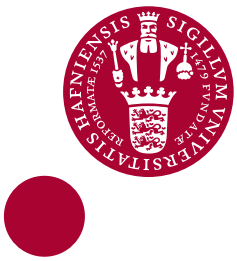

Timescales for charge transfer based operations on Majorana systems

Seoane Souto, R.; Flensberg, K.; Leijnse, M.

Published in:
Physical Review B

DOI:
10.1103/PhysRevB.101.081407

Publication date:
2020

Document version
Publisher's PDF, also known as Version of record

Rapid Communications

Timescales for charge transfer based operations on Majorana systems

R. Seoane Souto,[1,2] K. Flensberg,[1] and M. Leijnse[1,2]
[1]*Center for Quantum Devices, Niels Bohr Institute, University of Copenhagen, DK-2100 Copenhagen, Denmark*
[2]*Division of Solid State Physics and NanoLund, Lund University, Box 118, S-22100 Lund, Sweden*

(Received 25 October 2019; revised manuscript received 20 January 2020; accepted 22 January 2020; published 18 February 2020)

In this Rapid Communication we analyze the efficiency of operations based on transferring charge from a quantum dot (QD) to two coupled topological superconductors, which can be used for performing non-Abelian operations on Majorana bound states (MBSs). We develop a method which allows us to describe the full time evolution of the system as the QD energy is manipulated. Using a full counting statistics analysis, we set bounds to the operation timescales. The lower bound depends on the superconducting phase difference due to a partial decoupling of the different MBS parity sectors, while the upper bound is set by the tunneling of quasiparticles to the MBSs. Using realistic parameters, we find the existence of a regime where the operation can be carried out with a fidelity close to unity. Finally, we propose the use of a two-operation protocol to quantify the effect of the dephasing and accumulated dynamical phases, demonstrating their absence for certain superconducting phase differences.

DOI: 10.1103/PhysRevB.101.081407

I. INTRODUCTION

Prediction of the existence of Majorana bound states (MBSs) at the ends of a topological superconductor (TS) has given hope of observing non-Abelian statistics (for recent reviews, see [1–5]), which can potentially be used for topological quantum computation [6]. Earliest evidence of their existence was based on local probes coupled to the ends of a TS, showing the buildup of a zero-bias peak, firstly measured in Ref. [7]. More recently, some experiments have shown additional pieces of evidence consistent with the presence of MBSs in proximity-induced superconducting devices such as the zero-bias conductance quantization [8,9], interferometry signatures [10], exponential scaling with length in Coulomb blockaded islands [11], and interactions between zero-energy states and quantum dot (QD) orbitals [12].

However, an unambiguous proof of their topological origin would rely on the demonstration of their non-Abelian statistics. Some previous theoretical proposals in this direction were based on a spatial exchange of MBSs in a multiterminal device [13] and others used tunneling or Coulomb blockade to manipulate the ground-state manifolds [14–16]. Alternatively, signatures of the predicted non-Abelian statistics can emerge after a sequence of manipulations of the quantum state of a set of MBSs, using charge-transfer-based operations of QDs coupled to TSs [17]. The dependence of the final state on the order in which the operations are performed would reveal the non-Abelian nature of MBSs.

In this work, we analyze the efficiency of the charge-transfer operation of a QD coupled to two TS electrodes [17], schematically represented in Figs. 1(a) and 1(b). During the operation, the QD level energy is swept from negative to positive energies well outside the superconducting gap, as illustrated in Fig. 1(c). As a consequence, the electron initially residing in the QD is transferred to the TSs. In a successful operation the QD empties into the MBSs [solid arrows in Fig. 1(d)]. As an example, starting from an initial $|p_L, p_R\rangle_i = |1, -1\rangle$ state (where ± 1 means even/odd MBS parity of one of the leads), it evolves to a superposition between $|1, 1\rangle$ and $|-1, -1\rangle$ after a successful operation, with weights proportional to the tunneling amplitudes to the right and left TSs, respectively, and a relative phase given by the superconducting phase difference. Differently from Ref. [17], we consider the full time dynamics of the system, taking also into account the degrees of freedom from the continuum of states. This allows us to analyze various sources of errors such as the nonadiabatic effects, which can make the QD charge relax [dashed arrows in Fig. 1(d)], and the role of excited quasiparticles above the superconducting gap, which can produce undesired parity changes.

In order to analyze the change in the MBSs parity, we use a full counting statistics formalism which allows us to keep track of the transferred electrons in the junction. For experimentally accessible temperatures, we find an optimal manipulation rate window where operations can be performed with high fidelity. We propose a protocol based on two charge-transfer operations, where the QD level returns back to its original value at the final time, as a way of quantifying the influence of dephasing and accumulated dynamical phases. Deviations between the initial and final states provide a measurement of the effect of the different sources of errors.

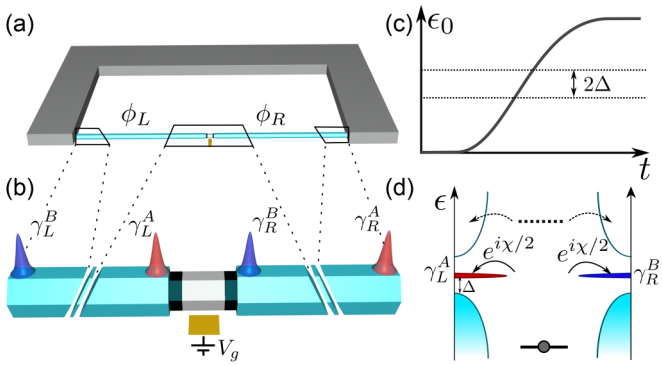

FIG. 1. (a) Schematic representation of the device consisting of two long TS wires (blue) embedded into a superconducting loop. (b) Enlarged representation of the ends of the wires, which host MBSs ($\gamma_{L,R}^{A,B}$), and the QD used for the operations. (c) Time evolution of the QD energy level. (d) Energy representation, where curved arrows represent the processes of the electron tunneling to the MBSs (solid lines) or to the continuum of states (dashed lines) during the manipulation of the QD level energy (thick horizontal line).

II. THEORETICAL FRAMEWORK

We consider two TSs coupled to a QD schematically shown in Figs. 1(a) and 1(b) and described by the Hamiltonian

$$H = H_L + H_R + H_{\rm QD} + H_T. \tag{1}$$

Here, $H_\nu = \sum_n (\hat{\Psi}^\dagger_{n,\nu} \hat{h}_{0,\nu} \hat{\Psi}_{n,\nu} + \hat{\Psi}^\dagger_{n+1,\nu} \hat{h}_{s,\nu} \hat{\Psi}_{n,\nu})$ is the Hamiltonian of the TSs, described by the spinless Kitaev Hamiltonian [18], where $\hat{\Psi}_{n,\nu} = (c_{n,\nu}, c^\dagger_{n,\nu})^T$ is the Nambu spinor, with $c_{n,\nu}$ ($c^\dagger_{n,\nu}$) being the annihilation (creation) operators on site n of electrode $\nu = L, R$. The first term describes the on-site energy, $\hat{h}_{0,\nu} = -\mu\hat{\tau}_z/2$. The second term contains information about the hopping between neighboring sites and p-wave superconducting correlations, $\hat{h}_{s,\nu} = -t_0\hat{\tau}_z/2 + i\Delta\hat{\tau}_y/2$, with t_0 the normal hopping between neighbors and Δ the induced superconducting gap, taken to be the same in both electrodes for simplicity. The Hamiltonian of the spinless QD is given by $H_{\rm QD} = \hat{\Psi}^\dagger_d \hat{h}_0 \hat{\Psi}_d$, where $\hat{h}_0 = \epsilon_0(t)\hat{\tau}_z/2$ and $\hat{\Psi}_d = (d, d^\dagger)^T$. The time-dependent QD level energy, $\epsilon_0(t)$, evolves during the considered operation from the initial value ϵ_i to the final one ϵ_f (with $|\epsilon_i|, |\epsilon_f| \gg \Delta$). For simplicity, $\epsilon_0(t)$ is assumed to evolve linearly in time close to the superconducting gap with a slope r, as illustrated in Fig. 1(c). Finally, $H_T = \sum_\nu (\hat{\Psi}^\dagger_{0,\nu} \hat{h}_{T_\nu} \hat{\Psi}_d + \text{H.c.})$ describes the tunneling of electrons between the QD and the closest site of the two TSs with $\hat{h}_{T_\nu} = t_\nu \hat{\tau}_z e^{i\hat{\tau}_z\phi_\nu/2}$, where $\phi = \phi_L - \phi_R$ determines the superconducting phase difference between the leads. The tunneling rates are defined as $\Gamma_\nu = \pi(t_\nu)^2\rho_F$, with $\Gamma = \Gamma_L + \Gamma_R$ and ρ_F being the normal density of states at the Fermi level, taken as $\rho_F = 1/\Delta$.

The dynamics of the system during an adiabatic operation is accurately described by a low-energy model, which only considers the MBSs in the leads. It is described by the Hamiltonian

$$H_{\rm LEM} = H_{\rm QD} + H_{T,\rm MBS}, \tag{2}$$

where $H_{T,\rm MBS} = V_L \gamma_L^A e^{i\phi_L/2} d + V_R \gamma_R^B e^{i\phi_R/2} d + \text{H.c.}$ is the tunneling Hamiltonian, with $V_\nu = t_\nu \rho_F \Delta$. Here, $\gamma_L^A = c_{0,L} + c^\dagger_{0,L}$ and $\gamma_R^B = i(c_{0,R} - c^\dagger_{0,R})$ are the MBS operators at the closest end to the QD of the left and right TS [see Fig. 1(b)].

We use the nonequilibrium Green's function (NEGF) formalism to access the system state. In the time-dependent regime, the inverse QD NEGF is given by

$$G^{-1}(t,t') = g_0^{-1}(t,t') - \Sigma(t,t'), \tag{3}$$

where g_0^{-1} represents the inverse QD Green's function in the Keldysh-Nambu space [19–21] and Σ the tunneling self-energy. The self-energy can be decomposed into two contributions, $\Sigma = \Sigma_M + \Sigma_c$, describing the coupling to the MBSs and the continuum of states, respectively [expressions are given in the Supplemental Material (SM) [22]]. For simplicity, we consider a sudden connection between the QD and the electrodes at $t = 0$, such that the charge state of the QD and the parity state of the electrodes are initially well defined. We have checked that the connection process does not affect the initial parity state of the MBSs for an initial level position $|\epsilon_i| \gg \Delta$.

The problem is solved in the time domain by discretizing the Keldysh contour and numerically inverting Eq. (3). Information about the mean properties of the system can be extracted from the QD NEGFs. For instance, the average parity of each MBS can be obtained as $\langle p_\nu \rangle = i\langle \gamma_\nu^A \gamma_\nu^B \rangle$ (details are provided in the SM [22]).

In contrast, from the mean values obtained from the NEGFs of Eq. (3) it is not possible to extract the probability of a successful operation. This information can instead be obtained by projecting the number of electrons transferred between the QD and the MBSs using a full counting statistics analysis. This information is encoded in the generating function

$$Z(\chi,t) = \left\langle T_C \exp\left[-i \int_C dt' \sum_\nu H_{T,\chi}(t') \right] \right\rangle_0, \tag{4}$$

where the average is taken over the decoupled system and the counting field, χ, is a phase factor used to count tunneling electrons. It enters into the tunneling amplitudes as $\hat{h}_{T_\nu,\chi_\nu} = \hat{h}_{T_\nu} e^{i\tau_z^K(\hat{\tau}_0+\hat{\tau}_z)\chi_\nu/2}$, where τ_z^K is the Pauli matrix in Keldysh space, indicating the change on the counting field sign between the two Keldysh branches. We consider the counting field acting only for electrons tunneling between the QD and the MBSs, as illustrated in Fig 1(d) (and not between the QD and the quasiparticle states outside the gap), and take $\chi_L = \chi_R = \chi/2$, which projects the wave function onto a state with well-defined joint parity of left and right MBSs.

The GF can also be written as $Z(\chi,t) = \sum_n \mathcal{P}_n(t) e^{in\chi}$, where $\mathcal{P}_n$ is the probability of transferring n charges between the QD and the MBSs after a time t. Note that at $\chi = \pi$ the GF describes the MBSs parity change. In the Keldysh-Nambu space, the GF can be computed as a Fredholm determinant [19,20]

$$Z(\chi,t) = \frac{\det\left[g_0^{-1} - \Sigma(\chi)\right]}{\det\left[g_0^{-1} - \Sigma(\chi=0)\right]}. \tag{5}$$

The probability of a change of the joint MBS parity is described by the generating function as $P(t) = [1 - Z(\chi = \pi, t)]/2$, which is also the probability for the QD charge to

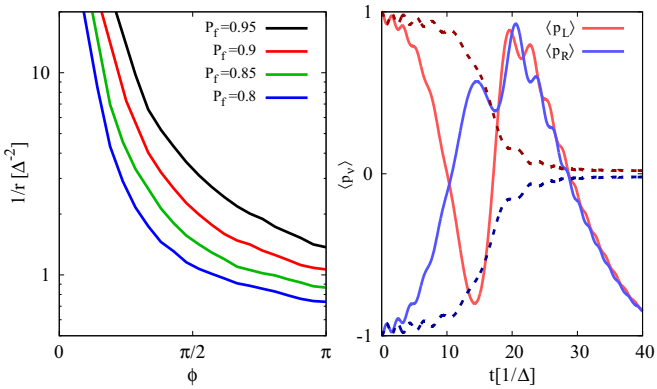

FIG. 2. Left panel: Dependence of the inverse of the operation rate as a function of the superconducting phase for different P_f values. Right panel: average parity of left and right MBSs during an operation with $r = \Delta^2/4$. We consider two different phases: $\phi = \pi/2$ (solid lines) and $\phi = \pi$ (dotted lines). In both cases we take $\Gamma_L = \Gamma_R = 0.15\Delta$ and temperature $T = 0$.

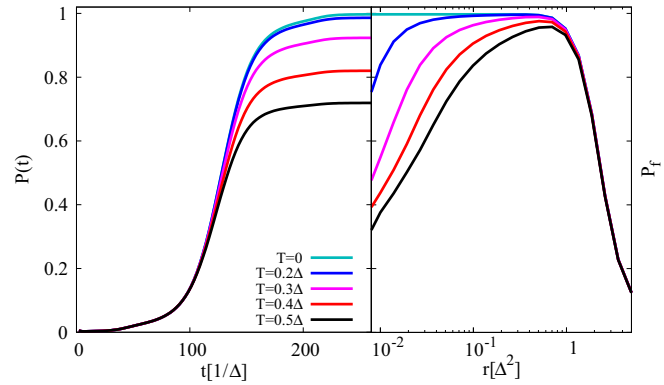

FIG. 3. Temperature dependence of the MBSs parity change probability, showing the time evolution (left panel) and the long-time limit as a function of the rate (right panel). Parameters are the same as in Fig. 2 with $\phi = \pi$.

be transferred to the MBSs. P saturates for $|\epsilon_0(t)| \sim 10\Gamma$ to a value P_f, leading to a total operation time $t \approx 20\Gamma/r$.

III. RESULTS

In this section we analyze the success probability of the charge-transfer-based operation on the system sketched in Figs. 1(a) and 1(b). We consider an initially well-defined MBS parity on both sides, choosing without loss of generality $|p_L, p_R\rangle_i = |1, -1\rangle$ as the initial MBS parity state. A successful operation in which the QD charge is efficiently transferred to the MBSs [solid arrows in Fig. 1(d)] leads to a change of the total MBS parity state (from odd to even in our case), leading to a final state $|p_L, p_R\rangle_f = (V_R e^{i\phi_R/2}|1, 1\rangle + V_L e^{i\phi_L/2}|-1, -1\rangle)/\sqrt{V_L^2 + V_R^2}$. As discussed below, this is only true for $\phi = (2n+1)\pi$.

In the left panel of Fig. 2 we show the dependence of the inverse manipulation rate $(1/r)$ on the superconducting phase difference for different values of P_f. As shown, the rate needed for a given P_f depends strongly on ϕ, becoming optimal (thus, minimizing operation times) for $\phi = (2n+1)\pi$. At $\phi = 2n\pi$ the time of the operation diverges due to the formation of a dark state preserving the total MBS parity state for $V_L = V_R$ and for any ϵ_0 value, setting a limit $P_f = 0.5$ for adiabatic operations. The dark state is given by $(|1, -1\rangle + i|-1, 1\rangle)/\sqrt{2}$ for the odd MBS parity sector and $(|1, 1\rangle + i|-1, -1\rangle)/\sqrt{2}$ for the even one. For $V_L \neq V_R$ the even and odd MBS parity sectors are no longer decoupled, although the value of r needed for reaching a P_f close to unity becomes strongly dependent on the asymmetry between the left and right tunneling rates close to $\phi = 2n\pi$.

In the right panel of Fig. 2 we show the average parity of the left and right MBSs for an adiabatic r value where $P_f \approx 1$ and two different superconducting phases. As shown, for $\phi = \pi \pmod{2\pi}$ $\langle p_L\rangle$ and $\langle p_R\rangle$ tend to 0 at long times, consistent with the convergence to the expected final state after the operation. In contrast, for $\phi \neq (2n+1)\pi$ the average parities exhibit oscillations during the manipulation, which leads to a dependence of the final state on the details of the operation. These oscillations are due to the breaking of degeneracy between the even and odd parity states of the nonlocal fermion formed by the left and the right MBSs, as shown in the SM [22]. For $\phi = (2n+1)\pi + \delta\phi$ the period of the oscillations is given by $\sqrt{\epsilon_0^2 + 4(V_L^2 + V_R^2)}/(4V_L V_R \delta\phi)$ with $\delta\phi \ll 1$. This illustrates the importance of having an accurate control on the superconducting phase difference. Additional oscillations are observed after the operation (for $|\epsilon_0| \gg \Delta$) with a period given by $\epsilon_0/[4V_L V_R \cos(\phi/2)]$. It is worth commenting that the same behavior is observed in the case in which the QD is coupled to the same Majorana operators (either γ^A or γ^B) at the left and right sides, as considered in Ref. [17], by shifting the superconducting phase difference value by π. In the following we will focus on the $\phi = (2n+1)\pi$ situation, where the parity oscillations are absent and P_f quantifies the success probability of the charge-transfer operation.

The analysis performed above would indicate that the choice of slower rates tends to improve the success probability. However, some additional processes can affect the operation fidelity for adiabatic rates, such as the decaying of excited quasiparticles into the MBSs, which lead to uncontrolled parity changes. First estimations have shown that these events happen in the millisecond timescale in a trivial wire, i.e., without MBSs [23]. Processes involving the decaying of quasiparticles directly into the MBSs will be disregarded in the following. Instead we consider the timescales for quasiparticles tunneling between the continuum and the MBSs mediated by the QD during the charge-transfer-based operation which, as it turns out, can be much shorter (see Fig. 3). At a finite T, there is a density of quasiparticles excited above the superconducting gap. For small T, the number of quasiparticles is exponentially suppressed and the manipulation can be performed with a high success probability, as illustrated by the blue curves in the left panel of Fig. 3. However, when the temperature increases, P_f drops for adiabatic rates. This is better illustrated in the right panel of Fig. 3 where we show that P_f exhibits a maximum, decreasing for small r values, due to the tunneling of thermally excited quasiparticles to the QD.

For small temperatures ($T \lesssim 0.2\Delta$), the system exhibits a range of r values where P_f is close to unity. We observe

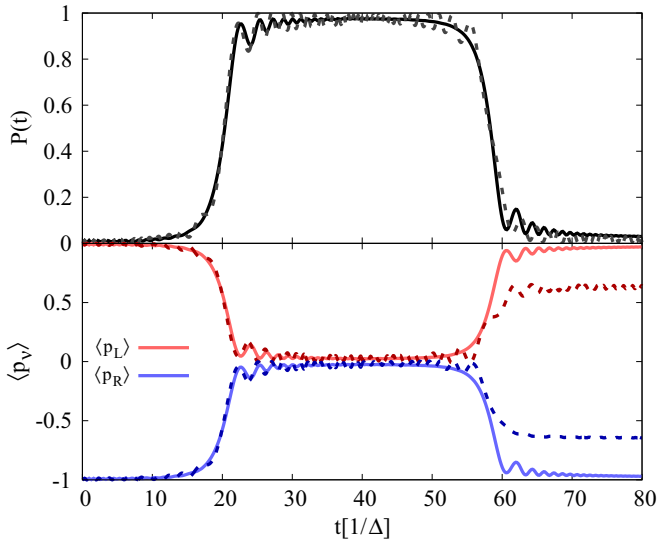

FIG. 4. Results for a double charge-transfer operation where the QD level returns to its initial value at the final time. The solid curves describe the coherent dynamics while the dashed ones illustrate the effect of a randomly distributed phase, $\xi \in [-\pi/2, \pi/2]$, introduced in the quantum state after the first manipulation, using the low-energy Hamiltonian of Eq. (2). Upper panel: probability of total MBS parity change. Lower panel: left and right MBS parity. The parameters are the same as in Fig. 2 with $\phi = \pi$ and $r = \Delta^2/2$.

that the decay point of P_f for decreasing r values scales linearly with the density of thermally excited quasiparticles. It allows us to estimate an optimal window for the rate using experimentally relevant parameters where $k_B T/\Delta \sim 0.1$, finding $r/\Delta\Gamma \sim 10^{-4}$–$10^{-1}$. This leads to an estimated manipulation timescale of the order of 0.1 μs to 0.1 ns for V_L and V_R smaller but of the same order of magnitude as Δ. The upper bound has been estimated considering an equilibrium distribution of excited quasiparticles with energies larger than the superconducting gap. It can be significantly reduced if a higher density of these quasiparticles is found in the TSs.

While Figs. 2 and 3 describe the probability of changing the parity of the MBSs, they do not contain information about dephasing or the accumulation of dynamical phases. These effects can be generated by high-order processes involving the tunneling of electrons between the QD and the continuum of states. In order to quantify the dephasing, we suggest two charge-transfer operations, where the QD level energy is swept from ϵ_i to ϵ_f and then back to ϵ_i. The results of this protocol are shown in Fig. 4 for a situation where a high P_f is observed in the right panel of Fig. 3 (solid lines). In the top panel of Fig. 4 we show the change of the joint MBS parity, which evolves to almost 1 after the first manipulation and returns back to almost 0 when the QD level energy returns to its original value (solid line). The lower panel of Fig. 4 shows the average parity values of the left and right MBS pairs during the operation, confirming that the parity of each electrode returns back to its original value after the second operation (solid lines). We have also verified that the final state of the electrodes does not degrade if different adiabatic rates are considered for the two manipulation processes, indicating the absence of uncontrolled dynamical phases for $\phi = \pi$ (mod 2π).

The dashed lines in Fig. 4 illustrate the effect of an accumulation of uncontrolled phase factors after the first operation, which we simulate using a randomly distributed phase ξ in a given interval. Therefore, the state after a successful first operation is $\propto (V_R e^{i\phi_R/2}|1,1\rangle + V_L e^{i(\phi_L/2+\xi)}|-1,-1\rangle)$. This is analyzed using the low-energy model described in Eq. (2), which accurately describes the system adiabatic evolution. While the total MBS parity change is not affected by the inclusion of randomly distributed phase ξ (top panel of Fig. 4), the individual parities of the electrodes do not return back to their original values. Instead, they approach $\langle p_v\rangle = 0$ in the limit the introduced phase factor is completely random. Therefore, the difference between the initial and final parity states, $\delta(\langle p_v\rangle) = \langle p_v\rangle_f - \langle p_v\rangle_i$, quantifies the accumulated error in the whole process. The error on a single manipulation can be estimated as $1 - \sqrt{1 - |\delta(\langle p_v\rangle)|}$ in the regime where no other errors occur between the first and the second operation.

IV. CONCLUSIONS

We have analyzed the efficiency of the charge-transfer-based operations of a QD coupled to two topological superconductors, setting bounds to its optimal timescales. We have found the optimal parameters where the final state after an adiabatic operation does not depend on the details of how it is performed. We have also analyzed the effects of imperfections in the system that affect the adiabatic operations, studying the effect of the excited quasiparticles above the superconducting gap at finite temperature, which leads to a lower bound to the manipulation rate. In the SM [22] we furthermore investigate the effects of an overlap between the MBS wave functions within a wire. We show that this leads to an upper bound on the operation timescale determined by the inverse of the difference between the overlap strength on both sides. Our results establish charge-transfer-based operations as a realistic alternative to experimentally probe the non-Abelian nature of MBSs.

ACKNOWLEDGMENTS

We acknowledge valuable contributions from A. Levy Yeyati and A. Martín-Rodero on the code development. We acknowledge funding from the Danish National Research Foundation. R.S.S. and M.L. acknowledge funding from QuantERA project "2D hybrid materials as a platform for topological quantum computing" and from NanoLund.

[1] J. Alicea, Rep. Prog. Phys. **75**, 076501 (2012).
[2] M. Leijnse and K. Flensberg, Semicond. Sci. Technol. **27**, 124003 (2012).
[3] C. Beenakker, Annu. Rev. Condens. Matter Phys. **4**, 113 (2013).
[4] R. Aguado, Riv. Nuovo Cimento **40**, 523 (2017).
[5] R. M. Lutchyn, E. P. A. M. Bakkers, L. P. Kouwenhoven, P. Krogstrup, C. M. Marcus, and Y. Oreg, Nat. Rev. Mater. **3**, 52 (2018).

[6] C. Nayak, S. H. Simon, A. Stern, M. Freedman, and S. Das Sarma, Rev. Mod. Phys. **80**, 1083 (2008).
[7] V. Mourik, K. Zuo, S. M. Frolov, S. R. Plissard, E. P. A. M. Bakkers, and L. P. Kouwenhoven, Science **336**, 1003 (2012).
[8] F. Nichele, A. C. C. Drachmann, A. M. Whiticar, E. C. T. O'Farrell, H. J. Suominen, A. Fornieri, T. Wang, G. C. Gardner, C. Thomas, A. T. Hatke, P. Krogstrup, M. J. Manfra, K. Flensberg, and C. M. Marcus, Phys. Rev. Lett. **119**, 136803 (2017).
[9] H. Zhang, C.-X. Liu, S. Gazibegovic, D. Xu, J. A. Logan, G. Wang, N. van Loo, J. D. S. Bommer, M. W. A. de Moor, D. Car, R. L. M. Op het Veld, P. J. van Veldhoven, S. Koelling, M. A. Verheijen, M. Pendharkar, D. J. Pennachio, B. Shojaei, J. S. Lee, C. J. Palmstrøm, E. P. A. M. Bakkers, S. D. Sarma, and L. P. Kouwenhoven, Nature (London) **556**, 74 (2018).
[10] A. M. Whiticar, A. Fornieri, E. C. T. O'Farrell, A. C. C. Drachmann, T. Wang, C. Thomas, S. Gronin, R. Kallaher, G. C. Gardner, M. J. Manfra, C. M. Marcus, and F. Nichele, arXiv:1902.07085.
[11] S. M. Albrecht, A. P. Higginbotham, M. Madsen, F. Kuemmeth, T. S. Jespersen, J. Nygård, P. Krogstrup, and C. M. Marcus, Nature (London) **531**, 206 (2016).
[12] M. T. Deng, S. Vaitiekenas, E. B. Hansen, J. Danon, M. Leijnse, K. Flensberg, J. Nygård, P. Krogstrup, and C. M. Marcus, Science **354**, 1557 (2016).
[13] J. Alicea, Y. Oreg, G. Refael, F. von Oppen, and M. P. A. Fisher, Nat. Phys. **7**, 412 (2011).
[14] J. D. Sau, D. J. Clarke, and S. Tewari, Phys. Rev. B **84**, 094505 (2011).
[15] T. Hyart, B. van Heck, I. C. Fulga, M. Burrello, A. R. Akhmerov, and C. W. J. Beenakker, Phys. Rev. B **88**, 035121 (2013).
[16] D. Aasen, M. Hell, R. V. Mishmash, A. Higginbotham, J. Danon, M. Leijnse, T. S. Jespersen, J. A. Folk, C. M. Marcus, K. Flensberg, and J. Alicea, Phys. Rev. X **6**, 031016 (2016).
[17] K. Flensberg, Phys. Rev. Lett. **106**, 090503 (2011).
[18] A. Y. Kitaev, Phys. Usp. **44**, 131 (2001).
[19] A. Kamenev, *Field Theory of Non-Equilibrium Systems* (Cambridge University Press, Cambridge, UK, 2011).
[20] R. S. Souto, A. Martín-Rodero, and A. L. Yeyati, Phys. Rev. Lett. **117**, 267701 (2016).
[21] R. S. Souto, A. Martín-Rodero, and A. L. Yeyati, Phys. Rev. B **96**, 165444 (2017).
[22] See Supplemental Material at http://link.aps.org/supplemental/10.1103/PhysRevB.101.081407 for details on the numerical methods used in this work, which includes Refs. [24–26]
[23] A. P. Higginbotham, S. M. Albrecht, G. Kirsanskas, W. Chang, F. Kuemmeth, P. Krogstrup, T. S. Jespersen, J. Nygård, K. Flensberg, and C. M. Marcus, Nat. Phys. **11**, 1017 (2015).
[24] A. Martín-Rodero and A. L. Yeyati, Adv. Phys. **60**, 899 (2011).
[25] A. Zazunov, R. Egger, and A. Levy Yeyati, Phys. Rev. B **94**, 014502 (2016).
[26] N. Bondyopadhaya and D. Roy, Phys. Rev. B **99**, 214514 (2019).